2011

Light propagation in biaxial nematic liquid crystal polymers using the finite-difference time-domain method

Choate, Eric P.; Zhou, Hong

Light propagation in biaxial nematic liquid crystal polymers using the finite-difference time-domain method

Eric P. Choate[1] and Hong Zhou

Department of Applied Mathematics, Naval Postgraduate School, Monterey, CA 93943

Abstract

We examine the propagation of electromagnetic waves across a liquid crystal polymer (LCP) domain using the finite-difference time-domain (FDTD) method. In the limit of perfect LCP alignment, the order parameter s approaches unity, and the LCP recovers a uniaxial alignment completely described by the major director **n** given by Leslie-Ericksen theory. We use a Doi-Marrucci-Greco tensor model formulation for the LCP orientation to examine the effect of less-than-perfect alignment. In a one-dimensional system with the orientation allowed to vary across the gap between two glass plates, we first examine uniaxial orientations for which $s<1$, and then we examine the effects of biaxial orientations, and in each case, we look at the role of using different anchoring directions at the two plates, which can induce deformations in the major director. Also, we examine oblate defect phases in which the sample is not isotropic but still fails to have a well defined major director.

Keywords: Liquid crystal polymers, Light propagation in anisotropic media, Finite-Difference Time-Domain method

Nomenclature

α = dimensionless strength of the DMG distortional elasticity potential
β = DMG biaxiality parameter
$\widetilde{\mathbf{D}}$ = rescaled electric flux
$\widetilde{\mathbf{E}}$ = rescaled electric field
$\boldsymbol{\varepsilon}$ = relativity permittivity tensor
$\varepsilon_{||}$ = extraordinary relativity permittivity constant
$\varepsilon_{\perp}$ = ordinary relativity permittivity constant
H = magnetic field
h = width of the gap between the two plates
M = second moment tensor from DMG theory
d_i = eigenvalues of **M**
m = the axis of symmetry of our idealized spheroidal molecules
n = major director from Leslie-Ericksen theory
$\mathbf{n}_1$ = major director from DMG tensor theory

[1] Corresponding author: Department of Applied Mathematics, Naval Postgraduate School, 833 Dyer Rd, Bldg 232, SP-250, Monterey, CA, 93943. Phone: 831-656-3247. Fax: 831-656-2355. Email: echoate@nps.edu.

$\mathbf{n}_2$= minor director from DMG tensor theory
N = DMG dimensionless concentration parameter
s = DMG order parameter
s_0 = DMG nematic equilibrium order parameter

Introduction

Liquid crystal displays have become commonplace due to the dynamic controllability of the anisotropic refractive indices of the liquid crystals. We wish to examine the effectiveness of an anisotropic liquid crystal layer as a defense against a laser weapon through mathematical modeling of the propagation of a beam through a liquid crystal layer. Usage of the Finite-Difference Time-Domain (FDTD) method for modeling light propagation in liquid crystal polymers (LCPs) is becoming more common [Hwang and Rey, 2005ab, 2006; Hwang et al, 2007; Kriezis and Elston, 1999, 2000]. This is due to its ability to handle spatial gradients in the molecular orientation better than previous methods.

These studies use Leslie-Ericksen (LE) theory [de Gennes and Prost, 1993] to model the molecular orientation. This theory describes the orientation with the major director **n**, a unit victor field that gives the average direction of the alignment of the axes of symmetry of the ensemble of liquid crystal molecules, which we idealize as rigid spheroids with no positional ordering of their centers of mass. Doi-Marrucci-Greco (DMG) theory, however, provides more degrees of freedom in the orientation field by using the second moment tensor **M** of an orientational probability density function as its primitive variable [Wang, 2002]. This provides both a full director frame and also information about how the orientation conforms to its average direction. The authors have previously examined the differences of the predictions of these two models in the context of flows of LCPs [Choate, et al, 2008, Choate, et al, 2010] and found that in some instances the predictions of the models can differ significantly. In this paper, we investigate the effect of the choice between these two orientational models on the propagation of a plane wave through an LCP domain.

The extra orientational information of the DMG model includes an order parameter s that that describes how strongly focused the orientation is around the major director. This effect applies to uniaxial distributions, which LE theory assumes, but in addition the DMG model includes a biaxial order parameter β that measures the attraction to a secondary direction in the plane transverse to the major director, which LE theory does not allow. These order parameters also allow for certain oblate defect structures in which the major director is not well defined, including the isotropic case, which cannot be represented by LE theory.

We examine two cases in which the extra degrees of freedom of the DMG model affect the predictions of the propagation of light in a different way than LE theory. In some contexts, the LE model can be thought of as the infinite concentration limit of DMG theory. We find that finite concentration effects can effectively lower the anisotropy of a uniaxial permittivity tensor.

We also explore the anchoring conditions on glass plates separated by an LCP layer that impose a twisting of the major director. LE theory predicts a helical structure of the director, which refracts light and allows it to pass through crossed polarized films on the plates, a mechanism exploited by liquid crystal displays. However, we find that for films thinner than a

certain critical thickness, the DMG model predicts a different type of behavior with two uniform directors extending the anchoring conditions halfway across the gap with the order parameters and the orientation becoming less focused around the anchoring director until reaching a defect layer in the middle of the gap, which allows the two mismatched directors to come together. Above the critical thickness, the DMG model predicts a helical structure very similar to the LE model. The helical structure can rotate the polarization of the incident beam while the defect structure cannot.

Theory

Figure 1 shows a cartoon of the geometry of our model system. Our incident beam is a monochromatic plane wave with wavelength of 633 nm. It propagates in the *z*-direction and is assumed to be ideally polarized with the electric field in the *x*-direction. The light passes through a lower supporting glass plate, and then through an LCP layer of width *h*, and then through a second glass plate. The inside surfaces of both plates are mechanically rubbed to establish anchoring conditions that align the major director and impose nematic order at the plates. Using different anchoring conditions on the two plates can generate orientational structures across the LCP domain with gradients in the optical axes that can refract light in a controlled way. We assume uniform anchoring in the *x*- and *y*-directions so that the structure

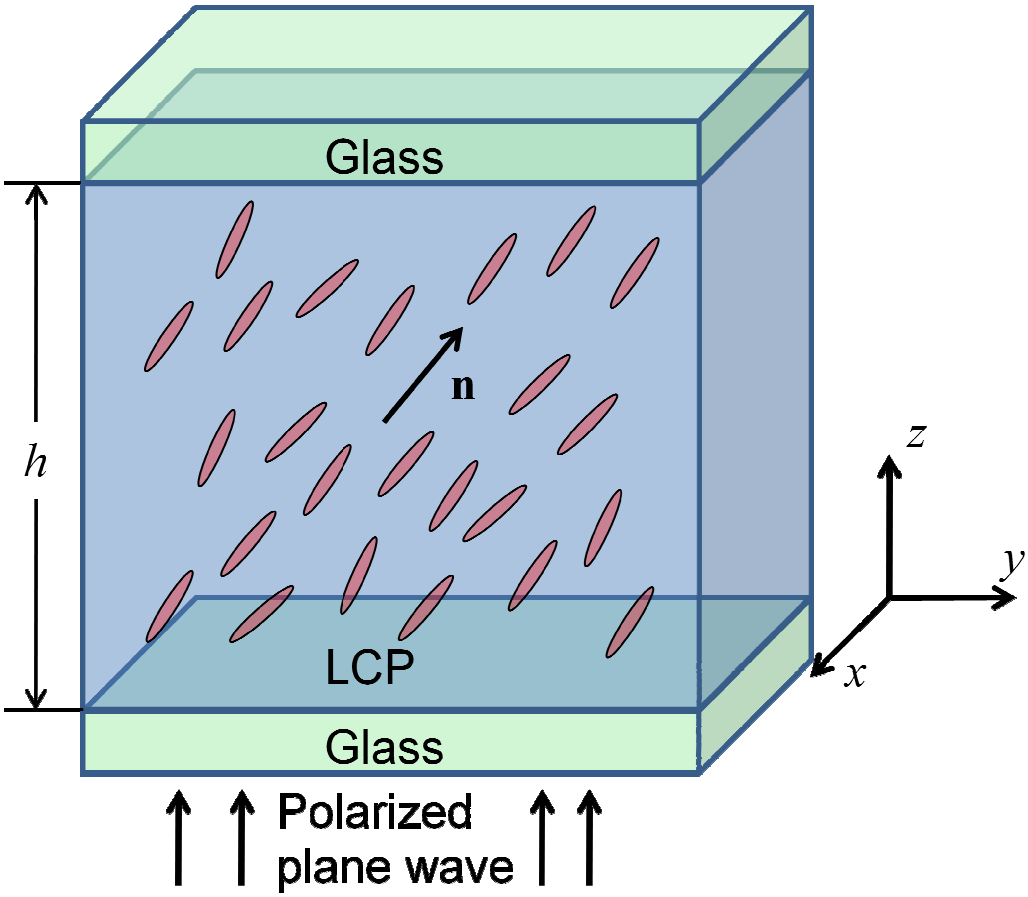

and the electrodynamics vary only in the z-direction. Our goal is to probe the differences in the light propagation due to the choice of model used to describe the structure of molecular alignment.

We assume that in both models that the molecular orientation is decoupled from the electromagnetic field so that the LCP is quenched into a solid phase before the light is passed through the sample. In LE theory, the orientation is captured by a single unit vector field $\mathbf{n}(\mathbf{x})$ called the major director, which is the average direction of the axes of symmetry $\mathbf{m}$ of the molecules located at $\mathbf{x}$. (The molecules are assumed to have a fore-aft symmetry and so there is no distinction between $\mathbf{n}$ and $-\mathbf{n}$.) In the absence of flow and neglecting reorientation by the electromagnetic field, $\mathbf{n}$ is given by the steady-state equation [de Gennes and Prost, 1993]

$$\mathbf{0} = (\mathbf{I} - \mathbf{nn})\cdot\nabla^2\mathbf{n}. \tag{1}$$

DMG theory describes the orientation through the second moment tensor $\mathbf{M} = \int_{\|\mathbf{m}\|=1} \mathbf{mm} f(\mathbf{m}, \mathbf{x}) d\mathbf{m}$ of an orientational probability density function f. Since $\mathbf{m}$ is a unit vector, $\mathbf{M}$ is symmetric and has trace 1, and so it has five independent components. Orientational information can be read from $\mathbf{M}$ by looking at its spectral representation

$$\mathbf{M} = s\left(\mathbf{n}_1\mathbf{n}_1 - \frac{\mathbf{I}}{3}\right) + \beta\left(\mathbf{n}_2\mathbf{n}_2 - \frac{\mathbf{I}}{3}\right) + \frac{\mathbf{I}}{3} \tag{2}$$

where the major director $\mathbf{n}_1$ is the eigenvector associated with the unique largest eigenvalue d_1. The order parameter $s = d_1 - d_3$ gives us a measure of how strongly ordered the system is. The biaxiality parameter $\beta = d_2 - d_3$ measures how far the alignment is from a uniaxial solution, and when $\beta > 0$, the eigenvector $\mathbf{n}_2$, or minor director, gives the most preferred direction of the projections of the molecules onto in the plane orthogonal to $\mathbf{n}_1$. The limit $(s = 1, \beta = 0)$ represents perfect alignment, in which case the tensor model reduces to the LE model. The steady-state equation for $\mathbf{M}$ is a balance of an excluded volume potential that imposes the nematic ordering if the concentration is strong enough and a distortional elasticity potential:

$$6\alpha[\mathbf{M} - \frac{\mathbf{I}}{3} - N(\mathbf{M}\cdot\mathbf{M} - \mathbf{M} : \mathbf{M}_4)] = \nabla^2\mathbf{M}\cdot\mathbf{M} + \mathbf{M}\cdot\nabla^2\mathbf{M} - 2\nabla^2\mathbf{M} : \mathbf{M_4} \tag{3}$$

where N is a dimensionless concentration parameter that measures the overall strength of the excluded volume potential, and $\alpha = \frac{8h^2}{NL^2}$, where the dimensionless strength of the distortional elasticity potential relative to the excluded volume effects for the persistence length L of the distortional elasticity potential [Wang, 2002]. We approximate the fourth moment tensor as $\mathbf{M}_4 \approx \mathbf{MM}$ to close the system on $\mathbf{M}$.

Equation (3) has an important degenerate equilibrium if there are assumed to be no spatial gradients. In the spectral variables (2), the order parameters are given by

$$0 = U(s) - \frac{2Ns\beta}{3}(s - \beta - 1)$$
$$0 = U(\beta) - \frac{2Ns\beta}{3}(\beta - s - 1) \tag{4}$$

where $U(s) = s(1 - N(1-s)(1+2s)/3)$. The solution is degenerate because any three constant orthonormal vectors define a set of eigenvectors. This eigenvector degeneracy can be broken by an external force such as a flow or in the present case by anchoring conditions at a hard wall boundary. There are two stable equilibrium order parameter solutions. The isotropic solution $(s,\beta) = (0,0)$ exists for any value of the concentration parameter *N*, but it is only stable if $N < 3$. This case has no molecular alignment and cannot be described by LE theory. The uniaxial nematic equilibrium solution $(s,\beta) = (s_0, 0)$ where $s_0 = (1 + 3\sqrt{1 - 8/(3N)})/4$ is defined if $N > 8/3$ and is stable if defined. There is a bistable region when $8/3 < N < 3$. As $N \to \infty$, $s_0 \to 1$, and so LE can be thought of as the infinite concentration limit. Figure 2 shows the stable equilibrium values of *s* as a function of *N*.

In this paper, we create one-dimensional structures between the two glass plates by

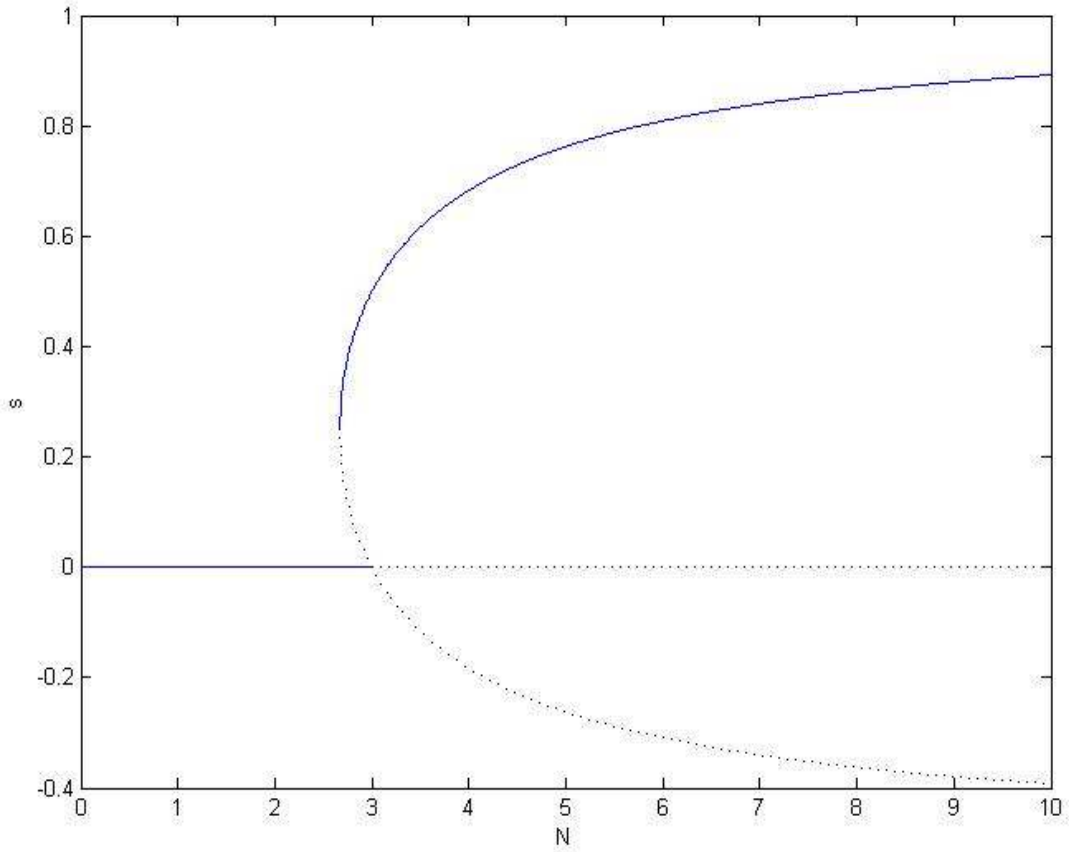

Figure 2. Equilibrium solutions for *s* from (4) as functions of the concentration parameter *N*. Solid curves are stable, dotted curves are unstable.

imposing the orientation at the plates. For the LE model, we simply impose the major directors $\mathbf{n}_{top}$ and $\mathbf{n}_{bottom}$ on the top and bottom plates, respectively. For the DMG model, we use these same major directors to construct uniaxial tensor anchoring conditions at the nematic equilibrium so that $\mathbf{M}_{top} = s_0(\mathbf{n}_{top}\mathbf{n}_{top} - \frac{\mathbf{I}}{3}) + \frac{\mathbf{I}}{3}$ and $\mathbf{M}_{bottom} = s_0(\mathbf{n}_{bottom}\mathbf{n}_{bottom} - \frac{\mathbf{I}}{3}) + \frac{\mathbf{I}}{3}$. If $\mathbf{n}_{top} = \mathbf{n}_{bottom}$, then the orientation is constant across the gap for both models.

Once the orientation is determined, the effect on the electrodynamics of the assumed nonmagnetic molecules lies in the relative permittivity tensor $\boldsymbol{\varepsilon}$. Both models have an extraordinary relative permittivity constant $\varepsilon_{||}$ for the direction parallel to the major director and an ordinary relative permittivity constant $\varepsilon_{\perp}$ for the orthogonal directions. The LE relative permittivity tensor is $\boldsymbol{\varepsilon}_{LE} = \varepsilon_{\perp}\mathbf{I} + \Delta\varepsilon\mathbf{nn}$, where $\Delta\varepsilon = \varepsilon_{||} - \varepsilon_{\perp}$, and the DMG relative permittivity tensor is $\boldsymbol{\varepsilon}_{DMG} = \varepsilon_{\perp}\mathbf{I} + \Delta\varepsilon\mathbf{M}$. We use the relative permittivity values $\varepsilon_{||}$ = 2.89 and $\varepsilon_{\perp}$= 2.25 from [Hwang and Rey, 2005ab, 2006]. We also assume the relative permeability is 1.

For the electric flux and field, we use the rescalings $\widetilde{\mathbf{D}} = \mathbf{D}/\sqrt{\varepsilon_0\mu_0}$ and $\widetilde{\mathbf{E}} = \mathbf{E}\sqrt{\varepsilon_0/\mu_0}$ so that Maxwell's equations with the linear constitutive equations become

$$\frac{\partial\widetilde{\mathbf{D}}}{\partial t} = \frac{1}{\sqrt{\varepsilon_0\mu_0}}\nabla\times\mathbf{H} \tag{5}$$

$$\widetilde{\mathbf{D}} = \boldsymbol{\varepsilon}\cdot\widetilde{\mathbf{E}} \tag{6}$$

$$\frac{\partial\mathbf{H}}{\partial t} = -\frac{1}{\sqrt{\varepsilon_0\mu_0}}\nabla\times\widetilde{\mathbf{E}} \tag{7}$$

where **D** is the electric flux, **E** is the electric field, **H** is the magnetic field, $\boldsymbol{\varepsilon}$ is the relative permittivity tensor of either the LE or DMG models, ε_0 is vacuum permittivity, and μ_0 is vacuum permeability. For simplicity, we drop the tildes for the rest of the paper.

We solve these numerically with a one-dimensional Finite-Difference Time-Domain scheme [Taflove and Hagness, 2005]. The electric field and flux and the relative permittivity are known on the space-time grid while the magnetic field is staggered on the half-grid. They are updated by

$$Dx_k^{n+1} = Dx_k^n - \frac{\Delta t}{\Delta z\sqrt{\varepsilon_0\mu_0}}(Hy_{k+1/2}^{n+1/2} - Hy_{k-1/2}^{n+1/2}), \tag{8}$$

$$\mathbf{E}_k^{n+1} = \boldsymbol{\varepsilon}_k^{-1}\cdot\mathbf{D}_k^{n+1}, \tag{9}$$

$$Hx_{k+1/2}^{n+3/2} = Hx_{k+1/2}^{n+1/2} + \frac{\Delta t}{\Delta z\sqrt{\varepsilon_0\mu_0}}(Ey_{k+1}^{n+1} - Ey_k^{n+1}), \tag{10}$$

where $\mathbf{D}_k^n = (Dx_k^n, Dy_k^n, 0)^T$ and $\mathbf{E}_k^n = (Ex_k^n, Ey_k^n, Ez_k^n)^T$ are the electric flux and field at $z = k\Delta z$ and $t = n\Delta t$, $\boldsymbol{\varepsilon}_k^{-1}$ is the inverse of the relative permittivity tensor at $z = k\Delta z$, and $\mathbf{H}_{k+1/2}^{n+1/2} = (Hx_{k+1/2}^{n+1/2}, Hy_{k+1/2}^{n+1/2}, 0)^T$ is the magnetic field at $z = (k+1/2)\Delta z$ and $t = (n+1/2)\Delta t$. The update equations for Dy_k^{n+1} and $Hy_{k+1/2}^{n+3/2}$ are similar. The update scheme preserves the divergence conditions $\nabla\cdot\mathbf{D} = 0$ and $\nabla\cdot\mathbf{H} = 0$ if they are satisfied by the initial conditions. Also, due to the assumption of no gradients in the *x*- and *y*-directions, *Dz* and *Hz* remain at their initial values, which we assume to be zero. However, due to the anisotropy in (9), *Ez* can be nonzero for some orientational structures. We use $h = 6.33$ μm, $\Delta z = 15.83$ nm, and $\Delta t = 2.64\times10^{-17}$ s.

The glass plates are assumed to be isotropic with a relative permittivity equal to the ordinary relative permittivity of the LCP. We use a scattered field/total field formulation to introduce the incident wave at the lower boundary of the total field region. We use uniaxial perfectly matched layers to truncate the computational domain without creating artificial reflections.

Comparison of Leslie-Ericksen and Doi-Marrucci-Greco Models

The easiest direct comparison of the two models is when the same tangential anchoring conditions are applied on each plate. In this case, the anchoring extends across the gap to give a constant uniaxial orientation throughout for both LE and DMG, which focuses the attention on the concentration effects of the DMG model through the equilibrium order parameter. For example, if we choose $\mathbf{n}_{top} = \mathbf{n}_{bottom} = (1,0,0)^T$, then LE theory gives

$$\boldsymbol{\varepsilon}_{LE} = \varepsilon_\perp \mathbf{I} + \Delta\varepsilon \mathbf{n}_{top}\mathbf{n}_{top} = \begin{bmatrix} \varepsilon_\parallel & 0 & 0 \\ 0 & \varepsilon_\perp & 0 \\ 0 & 0 & \varepsilon_\perp \end{bmatrix}, \tag{11}$$

and DMG theory gives

$$\boldsymbol{\varepsilon}_{DMG} = (\varepsilon_\perp + \Delta\varepsilon\frac{1-s_0}{3})\mathbf{I} + s_0\Delta\varepsilon \mathbf{n}_{top}\mathbf{n}_{top} = \begin{bmatrix} \varepsilon_\parallel^{\text{eff}} & 0 & 0 \\ 0 & \varepsilon_\perp^{\text{eff}} & 0 \\ 0 & 0 & \varepsilon_\perp^{\text{eff}} \end{bmatrix}. \tag{12}$$

Here we can identify effective extraordinary and ordinary relative permittivities for the DMG model as functions of the extraordinary and ordinary relative permittivities and the equilibrium order parameter as

$$\begin{aligned} \varepsilon_\parallel^{\text{eff}} &= \varepsilon_\parallel \frac{2s_0+1}{3} + \varepsilon_\perp \frac{2(1-s_0)}{3}, \\ \varepsilon_\perp^{\text{eff}} &= \varepsilon_\perp \frac{2+s_0}{3} + \varepsilon_\parallel \frac{1-s_0}{3}. \end{aligned} \tag{13}$$

Since s_0 is a function of the concentration parameter N, the effective relative permittivities are also functions of N, as shown in Figure 3. In the infinite concentration limit, the effective relative permittivities approach the LE values, which is consistent with the LE formulation being the infinite concentration limit of DMG theory. For finite concentrations in the nematic regime, the DMG model effectively decreases the uniaxial anisotropy, with $\Delta\varepsilon^{\text{eff}} = s_0(\varepsilon_{\parallel}^{eff} - \varepsilon_{\perp}^{eff}) = s_0\Delta\varepsilon$. In the isotropic regime, $s_0 = 0$ so that $\varepsilon_{\parallel}^{eff} = \varepsilon_{\perp}^{eff} = \frac{\varepsilon_{\parallel} + 2\varepsilon_{\perp}}{3}$ and there is no effective anisotropy. For the rest of this paper, we use $N = 6$, which makes $s_0 = 0.809$, $\varepsilon_{\parallel}^{eff} = 2.81$ and $\varepsilon_{\perp}^{eff} = 2.29$.

Now we turn our attention to twisted anchoring conditions. In this case we anchor the director to be parallel to the plates on both the top and the bottom, but on the bottom plate, it is parallel to the x-axis, and on the top it is parallel to the y-axis. We can parameterize the exact helical LE solution as $\mathbf{n} = (\cos\psi_{LE}(z), \sin\psi_{LE}(z), 0)^T$ for the director angle $\psi_{LE}(z) = \frac{\pi}{2}\frac{z}{h}$.

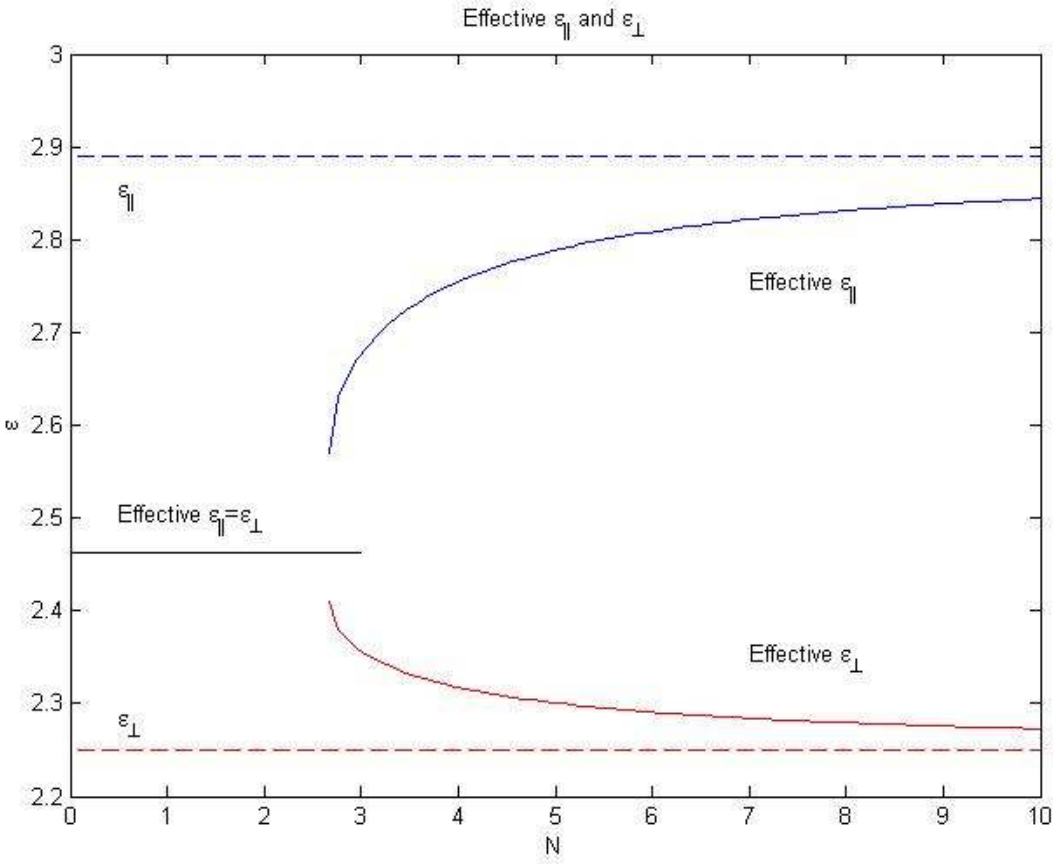

Figure 3. DMG Effective relative permittivities as functions of concentration parameter *N*

The behavior of the DMG model is more complicated. When the distortional elasticity parameter α in (3) is larger than a critical value, the behavior of the director is very similar to a uniaxial helical structure like the LE prediction. For N =6, this critical value is approximately 0.83, which would represent small gap widths when compared with the size of the molecules. For gaps wider than this, the order parameters are very close to their nematic equilibrium values with $s \approx s_0$ and $\beta \approx 0$, and the director angle is nearly linear and approximately equal to $\psi_{LE}(z)$.

Figure 4 shows the field components *Ex*, *Ey*, *Hx*, and *Hy* for the two models with $\alpha \approx 53$, which is greater than the critical value. For both models, the incoming wave is polarized to match the anchoring conditions with $\mathbf{n}_{bottom} = (1,0,0)^T$ so that initially *Ey* and *Hx* are zero. However, as it crosses the gap, the helical director rotates the polarization to be aligned with $\mathbf{n}_{top} = (0,1,0)^T$ so that *Ex* and *Hy* are now nearly zero. Due to the slightly weaker effective anisotropy, the DMG model does not damp *Ex* and *Hy* as strongly as the LE model.

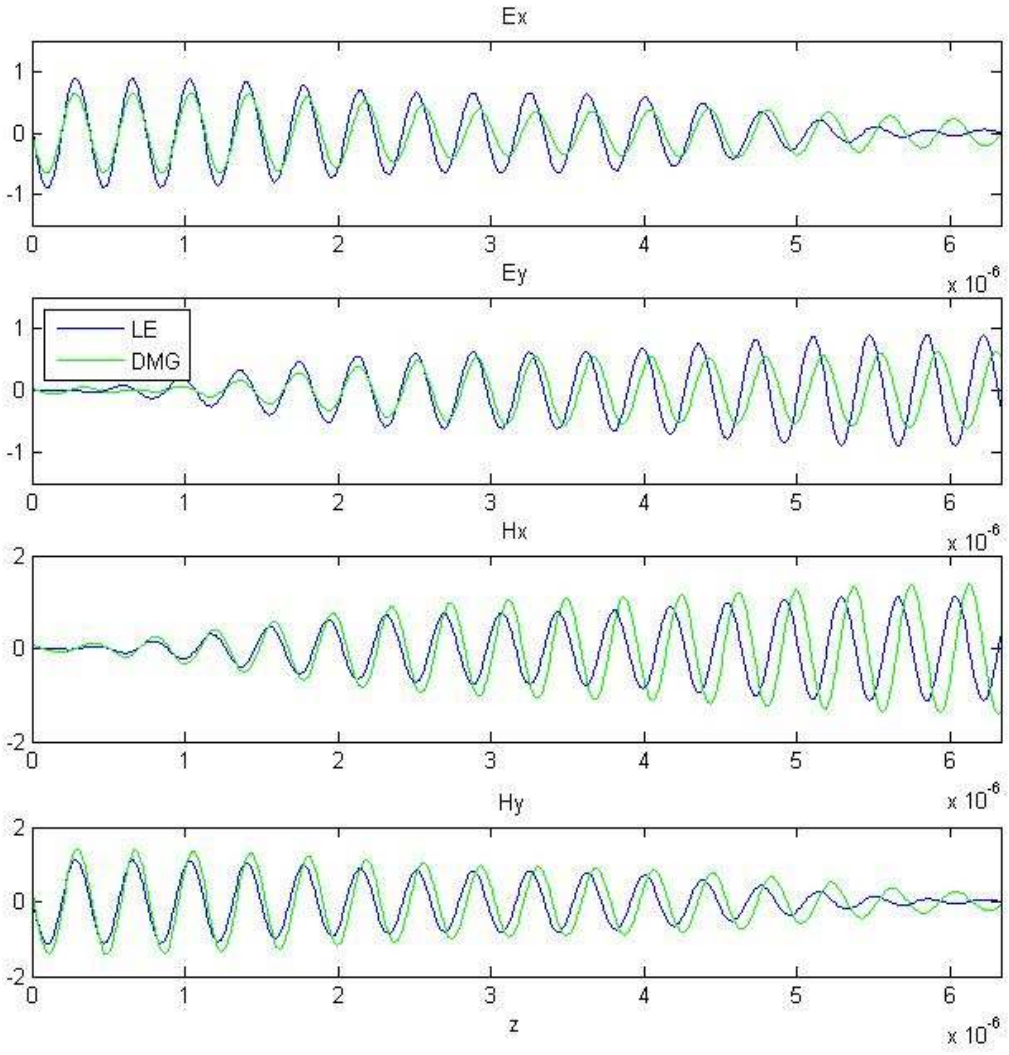

Figure 4 Electric and magnetic field for twisted anchoring above the critical value of α

The DMG model is significantly different for α below the critical value. The LE model is independent of α, and so its director angle is still the linear interpolation $\psi_{LE}(z) = \frac{\pi}{2}\frac{z}{h}$. However, as shown in Figure 5 for $\alpha = 0.66$, the DMG director angle is discontinuous, with

$$\psi_{DMG}(z) = \begin{cases} 0, & \text{if } 0 \le z < \frac{h}{2}, \\ \frac{\pi}{2}, & \text{if } \frac{h}{2} < z \le h. \end{cases}$$

This discontinuity corresponds to an order parameter oblate defect. As shown in Figure 6, the orientation becomes significantly biaxial away from the plates. At the midpoint, $s = \beta$, which implies that **M** fails to have a unique largest eigenvalue, and therefore no director can be chosen. There is no rotation in the eigenvector frame or the optical axes across the gap as in the helical LE model or the DMG model above the critical value of α, but instead the change is in which eigenvector is labeled as the major director.

There is a noticeable difference in the electromagnetic propagation. While the LE solution behaves similarly to the previous example by rotating the polarization, since the DMG

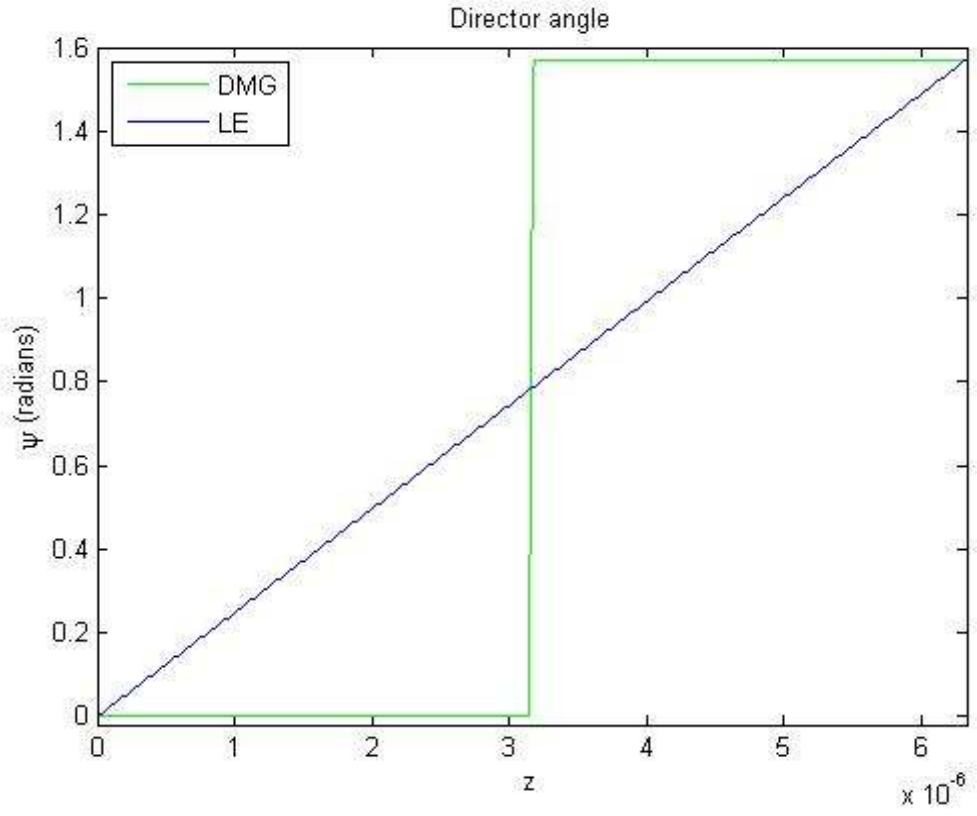

Figure 5 Director angles for α below the critical value

model has no rotation of the optical axes, there is no change in the polarization, and as shown in Figure 7, *Ey* and *Hx* remain zero.

We observed no significant differences between the Poynting vectors of the two models. In each case, the only nonzero component was the *z*-component, and the intensities were essentially the same.

We examined another case in which the DMG model has a similar generation of a defect below a threshold value of α. In the case of splay anchoring with anchoring parallel to the plate on the bottom $\mathbf{n}_{bottom} = (1,0,0)^T$ but orthogonal anchoring on the top plate $\mathbf{n}_{top} = (0,0,1)^T$. The LE case is again exactly solvable with $\mathbf{n}(z) = (\cos\theta_{LE}(z), 0, \sin\theta_{LE}(z))^T$ for the director angle $\theta_{LE}(z) = \frac{\pi}{2}\frac{z}{h}$. The DMG director is similar for large α but discontinuous for small α. However, we found no significant differences between the predictions of the light propagation between the two theories. In the splay case, the Poynting vector does have a nonzero *x*-component, but it is essentially the same for both theories, and we saw no significant differences in the intensity.

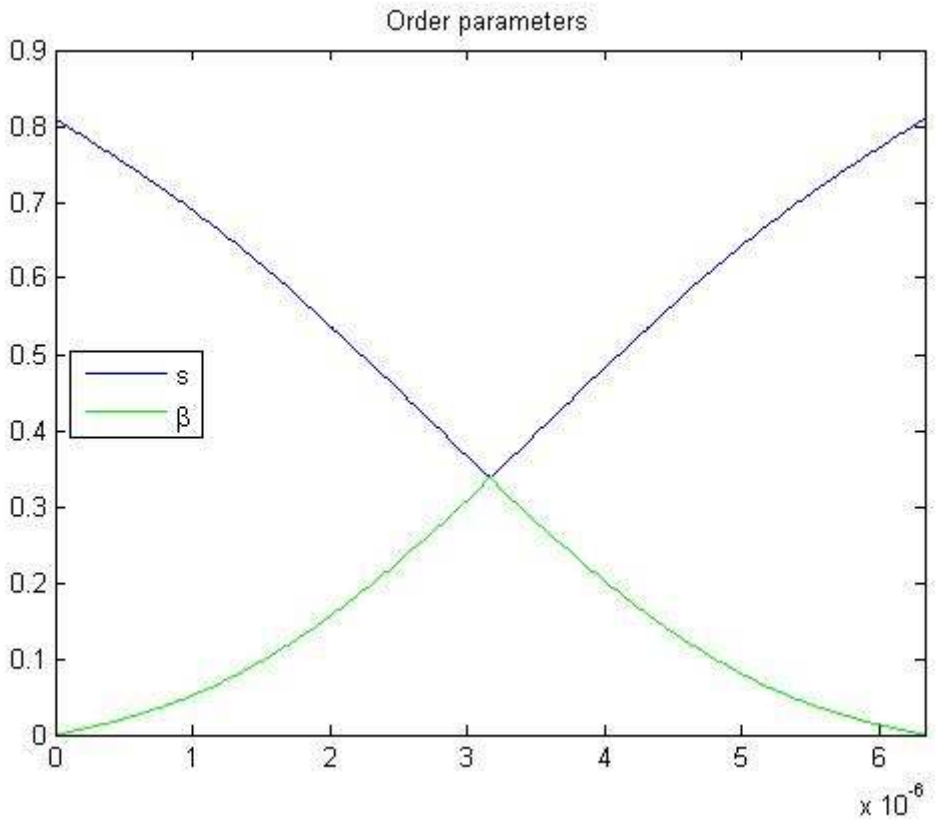

Figure 6. Order parameters for α below the critical value. There is an oblate defect when $s = \beta$

Conclusions and future work

We have examined the effect of the choice of modeling the orientation of a nematic liquid crystal polymer layer between with the major director **n** of Leslie-Ericksen theory or with the second moment tensor **M** from Doi-Marrucci-Greco theory. We found that the finite concentration effects of the DMG theory can effectively lessen the degree of anisotropy of a uniaxial distribution.

We probed thin-film situations in which the DMG model predicts an oblate order parameter defect layer halfway through the gap connecting two regions with a constant major

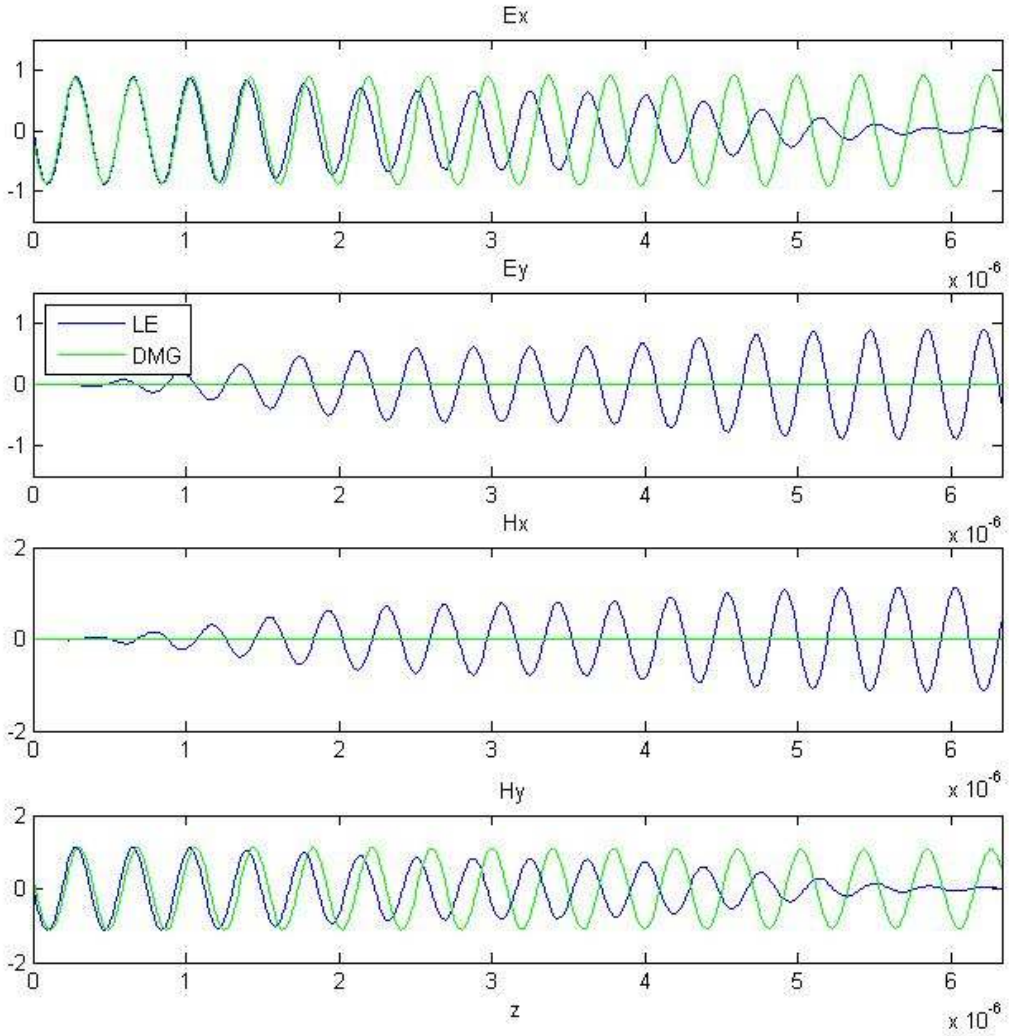

Figure 7. Electric and magnetic fields for below the critical value. The DMG model does not rotate the polarization like the LE model does.

director that matched the anchoring conditions at the nearer boundary. For twisted anchoring, this defect structure cannot rotate the polarization as the helical structure predicted by LE theory or DMG theory for wider gaps can.

Our next goal is to understand fully three dimensional orientational structures to see if they have similar dependence on the models, and then to examine the effect of the model choice on laser propagation.

As far as the intensity of the transmitted light is concerned, we found that the two models are very similar, even in the small gap regime when the orientation is different. This suggests that the overall differences between the models are not that significant for static orientations. Another way of looking at the two models is that LE theory is the limiting case of DMG theory as the timescale of rotational diffusion goes to zero. In the future, when we couple the orientation with the electromagnetic fields, larger nematic polymers for which the timescale of rotational diffusion is longer, we wish to revisit this issue.

The authors would like to thank the Office of Naval Research for the grant that supported this work.

References

Eric P. Choate, Zhenlu Cui, and M. Gregory Forest, Rheol. Acta. **47**, 223 (2008)

Eric P. Choate, M. Gregory Forest, and Lili Ju, Rheol. Acta. **49**, 335 (2010)

Pierre-Gilles de Gennes and Jacques Prost. *The Physics of Liquid Crystals*. (Oxford University Press, 1993).

Dae Kun Hwang and Alejandro D. Rey, Applied Optics. **44**, 4513 (2005a).

Dae Kun Hwang and Alejandro D. Rey, Liq. Cryst. **32**, 483 (2005b).

Dae Kun Hwang and Alejandro D. Rey, J. Opt. Soc. Am. A. **23**, 483 (2006).

Dae Kun Hwang, W.H. Han, and Alejandro D. Rey, J. Non-Newtonian Fluid Mech. **143**, 10 (2007).

Emmanouil E. Kriezis and Steve J. Elston, Optics Communications. **165**, 99 (1999).

Emmanouil E. Kriezis and Steve J. Elston, Optics Communications. **177**, 69 (2000).

Allen Taflove and Susan C. Hagness, *Computational Electrodynamics: The Finite-Difference Time Domain Method*, 3rd ed. (Artech House, Boston, 2005).

Qi Wang, J. Chem. Phys. **116**, 9120 (2002).